followed by translations only spinal cord registration. The difference between translations of vertebral and spinal cord registrations was analyzed (LR, AP, CC) as a measure for spinal cord movement within the CSF.
Results: Reproducibility of registration differences was good; on average 0.03±0.1 mm (LR, AP) and -0.2±0.4mm (CC) at T8. Opposing WFS (LR, AP) of 2x1.1 mm translate into corresponding registration differences of 1.7±0.1 mm in the T1 scans (Figure 1). Opposing 0.3 mm WFS for T2 scans could not be detected in registration differences. The cine MR images did not show spinal cord movement due to respiration (or respiration induced susceptibility changes). Positioning effects could not be distinguished within reproducibility for C7, T8 and L2. For L2, reproducibility was poorer in CC direction (SD 1.5 mm), possibly related to the more ambiguously defined equina cauda. In two participants, this caused spurious larger registration differences in AP and CC directions.

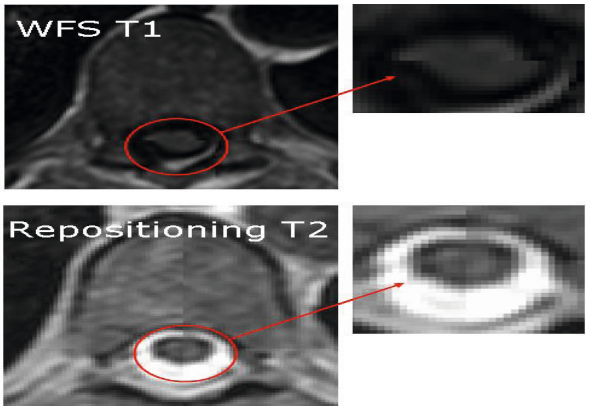

Figure 1. Respective influences of reversed WFS (above, T1 scan) and subject repositioning (below, T2 scan) on (perceived) spinal cord position inside the spinal canal. For both figures, a grey value match on the vertebral body was performed. The WFS is clearly visible in the spinal cord area, whereas no effect of repositioning can be observed.

Conclusions: MR properties and artefacts may influence perceived spinal cord location, which may be misleading in determination of spinal cord movement within the spinal canal. The robustness of the spinal cord position inside the spinal canal against respiration, repositioning and spine orientation suggests that the geometric accuracy of SRS for spinal oligometastasis remains uncompromised within a voxel.

PO-0859
Combined 18F-FDG and 18F-FLT PET/CT image characteristics to analyze esophageal squamous cell carcinoma stage
C. Ma[1], Y. Yin[1]
[1]*Shandong Cancer Hospital, Radiotherpy Oncology Physics, Jinan, China*

Purpose/Objective: The accuracy preoperative staging is crucial for esophageal carcinoma treatment. In this study we evaluate the capability of diagnostic information provided by ^{18}F-fluoro-deoxyglucose positron tomography/computed tomography and ^{18}F-fluorothymidine positron tomography/ computed tomography in esophageal squamous cell carcinoma(ESCC) staging. We also evaluate whether ^{18}F-FLT PET has the same performance in esophageal tumor stage comparing ^{18}F-FDG PET/CT. The advantages and disadvantages of ^{18}F-FDG PET/CT and ^{18}F-FLT/CT were preliminary investigated. Surgical resection was performed and relationship between PET/CT and tumor histology was explored to verify the recognition accuracy of preoperative PET/CT.
Materials and Methods: 26 patients with newly diagnosed ESCC underwent preoperative FDG FLT whole-body PET/CT separately. The correlation of the same patient's FDG, FLT SUV and texture parameters were investigated using Pearson correlation. Then all patients received surgical resection and pathological types were obtained. We compare the stage conducted based on PET/CT with pathology types to assessing the capability of PET/CT in the esophageal squamous cell carcinoma.
Results: FDG and FLT SUV have obvious correlation value r approximately 0.7 and p<0.01. However, only Entropy and Correlation have significant relationship between FDG and FLT PET images in texture parameters. In tumor stage SUV, texture parameters and shape feature have significant difference in corresponding histological tumor types and the results were verified accurate after operation.
Conclusions: The FDG and FLT PET scans have their own advantages for **ESCC** stage as both the radiotracers can reflect the proliferation of tumor cells. The PET/CT characteristics have their own moderately capability for different type esophageal staging.

PO-0860
ARTFIBio Project: quantifying tumour response voxel by voxel
A. Lopez Medina[1], D. Aramburu[1], M. Mera[1], L. Pereira[1], I. Landesa[2], V. Ochagavia[3], I. Nieto[3], J. Mañas[4], J.M. Nogueiras[5], V. Muñoz[3]
[1]*CHUVI, Medical Physics, Vigo (Pontevedra), Spain*
[2]*University of Vigo, Signal Theory and Communications, Vigo (Pontevedra), Spain*
[3]*CHUVI, Radiotherapy, Vigo (Pontevedra), Spain*
[4]*CHUVI, Radiology, Vigo (Pontevedra), Spain*
[5]*CHUVI, Nuclear Medicine, Vigo (Pontevedra), Spain*

Purpose/Objective: In recent years, there have been big improvements in the treatment of head and neck cancer (HNC), but local relapse rates are still higher than in other malignant pathologies. Functional studies from PET/CT and MRI are the most promising techniques for measuring tumour response and individualising treatment. In our hospital, we started a research project (2012-2014) focused on quantifying tumour response of HNC patients (#50) by serial PET/CT and MRI (Apparent Diffusion Coefficient - ADC). The aim of this paper is to present the methodology of the project as well as the preliminary results of the two first patients included in the study which are used to test the procedure.
Materials and Methods: For this study we select patients with 'oropharynx T3 and T4'. All of them will be treated with IMRT (S&S). The standard dose to the PTV is 66 Gy. The imaging protocol will be as follows:
-Pre-treatment: MRI study (1.5T Philips Achieva; single-shot echo-planar diffusion-weighted MR sequence with different b-values) and PET/CT study (Whole-body PET/CT,370 MBq of 18F-FDG; GE Discovery STE 16). These images will be used for contouring and treatment planning.
- First control (10 - 20 Gy): MRI diffusion study.
- Second control (20 Gy – 30 Gy): MRI diffusion study.
- Three months after the end of the treatment: PET/CT and MRI diffusion study.
For all the studies the patient is positioned using the RT immobilisation devices to ease image registration. The geometrical distortion on MRI images was checked. Therefore only the central slices showing low distortion were analyzed. For each patient and each set of images the ADC values, SUV, dose and HU per voxel (voxel size: 27 mm^3) were recorded of each volume.
Results:

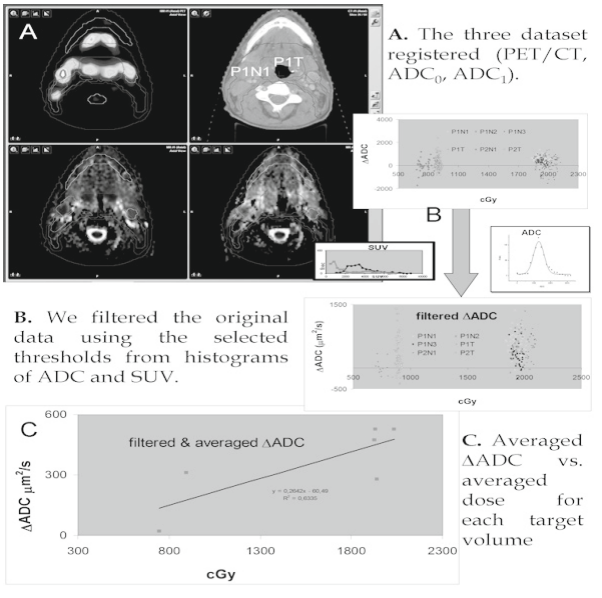

The average initial ADC value obtained for tumour and node volumes (Fig. 1A) of two first patients was $1{,}29 \cdot 10^{-3}$ mm^2/s and can be fitted to a Gaussian curve with a FWHM = $0{,}73 \cdot 10^{-3}$ mm^2/s (Fig. 1B). Histograms show a displacement to the right after radiotherapy sessions.
Considering only voxels with initial ADC in the range ± FWHM/2, and SUV >3 for the first patient, and >1 for the second one, and averaging for each volume, we obtain an increment of ΔADC with dose for both patients (Fig. 1B). The justification of different thresholds in SUV is because the differences in SUV histograms (Fig. 1B).

In the lower graph (Fig. 1C), we can observe an increase in ΔADC as dose increases, although the data are not relevant enough because of the few number of patients analyzed.
Conclusions: ADC maps can be used not only for treatment assessment, but also for quantification of tumour response voxel by voxel. Even more, the joint use of MRI diffusion data and PET/CT can be useful for delimiting the hypoxic areas, due to glucose consumption enhancement by Pasteur effect. The main weakness of this method is the rigid registration process, and non rigid registration algorithms are needed for the registration of highly distorted images from diffusion studies.
Supported by ISCIII Grant PI11/02035.

PO-0861
Prediction of normal tissue morbidity in radiotherapy of prostate cancer using motion inclusive dose distributions
M. Thor[1], L. Bentzen[2], L.B. Hysing[3], C. Ekanger[3], S.I. Helle[3], A. Karlsdóttir[3], L.P. Muren[1]
[1]*Aarhus University Hospital/Aarhus University, Dept. of Medical Physics Dept. of Oncology Dept. of Clinical Medicine, Aarhus, Denmark*
[2]*Aarhus University Hospital, Dept. of Oncology, Aarhus, Denmark*
[3]*Haukeland University Hospital, Dept. of Oncology and Medical Physics, Bergen, Norway*

Purpose/Objective: In radiotherapy (RT) of prostate cancer the key organs at risk (ORs) – the rectum and the bladder – display considerable motion, which may influence the dose/volume parameters predicting for morbidity. In this study we compare motion-inclusive doses to planned doses for the rectum and bladder and explore their associations with prospectively recorded morbidity.
Materials and Methods: The study included 38 prostate cancer patients treated with hypo-fractionated image-guided intensity-modulated RT that had an average of nine repeat CT scans acquired during treatment. These scans were registered to the respective treatment planning CT (pCT) followed by a new dose calculation from which motion-inclusive dose distributions were derived. The pCT volumes, the treatment course averaged volumes as well as the planned and motion-inclusive doses were associated with acute and late morbidity (morbidity cut-off: ≥ Grade 2).
Results: Acute rectal morbidity (observed in 29% of cases) was significantly associated with both smaller treatment course averaged rectal volumes (population median: 75 vs. 94 cm^{-3}) and the motion-inclusive volume receiving doses close to the prescription dose (2Gy-equivalent dose of 76 Gy).
Conclusions: Variation in rectum and bladder volumes leads to deviations between planned and delivered dose/volume parameters that should be accounted for to improve the ability to predict morbidity following RT.

PO-0862
Cross-institutional comparison of pharmacokinetic parameters from DCEMRI of cervical cancers: initial results
E. Andersen[1], J. Kallehauge[2], I.M. Jurgenliemk-Schulz[3], K. Tanderup[2], H. Lyng[4], E. Malinen[1]
[1]*Oslo University Hospital, Department of Medical Physics, Oslo, Norway*
[2]*Aarhus University Hospital, Department of Oncology, Aarhus, Denmark*
[3]*University Medical Center, Department of Radiotherapy, Utrecht, The Netherlands*
[4]*Oslo University Hospital, Department of Radiation Biology, Oslo, Norway*

Purpose/Objective: Biomarkers extracted from functional images may be subject to cross-institutional variations, and are thus in need of standardization. Pharmacokinetic parameters derived from dynamic contrast enhanced (DCE) MRI of cervical cancers have shown a predictive value in identifying patients at risk of relapse following radiotherapy. The aim of the current work was to compare pharmacokinetic parameters obtained from DCEMR images, acquired at different institutions, of patients with locally advanced cervical cancers.
Materials and Methods: DCEMRI images from 2 centers have so far been collected. At center 1 (Oslo University Hospital), 78 patients have been included. Here, DCEMRI was performed using Magnevist (Gadopentetate Dimeglumine) as contrast agent and an FSPGR sequence with temporal resolution of 15 s and spatial resolution of 0.8x0.8x5 mm at a 1.5T Signa Horizon LX scanner (GE Medical Systems). At center 2 (University Medical Center, Utrecht), 23 patients have been included. In this case, DCEMRI was performed using Magnevist and a 3D FLASH sequence with 2.4 s temporal resolution and spatial resolution 0.9x0.9x3mm at a 1.5T Gyroscan NT Intera scanner (Philips Medical Systems). Pharmacokinetic analysis with the 'Brix' model was performed in an identical manner for the two cohorts. The model analysis of the dynamic series was done voxel by voxel in the tumors, providing maps of the A_{Brix} (amplitude), k_{ep} and k_{el} parameters. The median of a given parameter was extracted for each patient, in addition to a relative measure of tumor heterogeneity (difference between 66th and 33rd percentile, divided by the median). Cohort data for each center was compared using Mann-Whitney tests. P-value<0.05 was considered statistically significant.
Results: The cohort-based median values for center 1 versus center 2 was 2.20 *vs* 3.41 (relative units), 1.59 *vs* 0.68 (min^{-1}) and 0.076 *vs* 0.080 (min^{-1}) for A_{Brix}, k_{ep} and k_{el}, respectively. For the heterogeneity measure, values obtained were 0.40 *vs* 0.55, 0.54 *vs* 0.99 and 1.10 *vs* 1.70, respectively. Non-significant differences were only found for median values of k_{el}.
Conclusions: Five out of six pharmacokinetic tumor parameters obtained from DCEMRI performed at the two different institutions were significantly different in this preliminary analysis, possibly pointing at differences in MR scanners and acquisition protocols. We aim at including patients from more institutions, at introducing the 'Tofts' pharmacokinetic model and at using reference tissue for normalization. Furthermore, data are to be analyzed in a multivariate setting, accounting for variations in stage, tumor volume and other relevant clinical factors.

PO-0863
Ultrasound IGRT: Deformable image registration of daily ultrasound images to derive daily CT images
S. van der Meer[1], D. Bouvy[2], B. Reniers[1], D. Fontanarosa[1], F. Verhaegen[1]
[1]*MAASTRO Clinic, GROW University Medical Centre Maastricht (Department of Radiation Oncology), Maastricht, The Netherlands*
[2]*Université Catholique de Louvain, École Polytechnique de Louvain, Louvain-la-Neuve, Belgium*

Purpose/Objective: Nowadays, quantitative 3D Ultrasound (US) Image Guided Radiotherapy (IGRT) systems are available which can assess absolute volumetric information on soft tissue. Acquiring daily US images is quick and imposes no extra radiation burden to the patient. For intramodality US systems only the reference CT (planning) image is available. Nevertheless, CT images for every treatment fraction would be useful, e.g. for dose recalculation, and assessing margins. To this end, deformable image registration (DIR) was applied to calculate the deformation field between reference and daily US images. This field was then applied to the reference CT.
Materials and Methods: To validate the procedure a deformable phantom was developed, existing of a PMMA box filled with demineralized water, containing two balloons filled with either saline solution or sunflower oil with a variable volume. Four different configurations were imaged with CT as well as US. Deformation fields are computed between several pairs of US images and then applied to the corresponding CT of the first US of the pair (see figure). This reconstructed new, matching CT for the second US is then compared to the real corresponding CT of the second US using the sum of squared differences (SQD) metric. The deformation fields are calculated using an elastic registration algorithm (REGGUI; morphons). The SQD metric was limited to the area where US information was available.